Kinetics of the $CH_2CH_2Cl \rightleftarrows C_2H_4 + Cl$ Reaction

Vadim D. Knyazev,* Ilia J. Kalinovski,† and Irene R. Slagle*

Department of Chemistry, The Catholic University of America, Washington, D.C. 20064

Received: October 27, 1998; In Final Form: March 2, 1999

The kinetics of the unimolecular decomposition of the CH_2CH_2Cl radical has been studied experimentally in a heated tubular flow reactor coupled to a photoionization mass spectrometer. Rate constants for the decomposition were determined in time-resolved experiments as a function of temperature (400−480 K) and bath gas density ([He] = (3−24) × 10^{16} atoms cm^{-3}). The rate constants are close to the low-pressure limit under the conditions of the experiments. Ab initio and master equation modeling are applied to analyze both the experimental data and literature data on the reverse reaction: the addition of Cl atom to ethylene. On the basis of the results of this modeling, parametrized expressions for the temperature and pressure dependencies of the rate constants for both the direct and the reverse reactions are provided.

I. Introduction

Reactions of chlorine atoms with hydrocarbons and chlorinated hydrocarbons, as well as their corresponding reverse reactions, are important constituents of overall kinetic mechanisms of such processes as incineration of halogenated hydrocarbons,[1] industrial thermal chlorination, and decay of Cl atoms and hydrocarbons in the atmosphere.[2] The reaction of Cl atom with the simplest unsaturated hydrocarbon, ethylene, has received wide experimental attention[3−12] (vide infra). Its main channel at low temperatures is the addition of the Cl atom to the double bond, producing the β-chloroethyl radical, CH_2CH_2Cl. There have been no prior experimental studies of the reverse reaction: the unimolecular decomposition of CH_2-CH_2Cl. Theoretical investigations of the reaction

$$CH_2CH_2Cl \rightleftarrows Cl + C_2H_4 \qquad (1,-1)$$

include ab initio studies of the potential energy surface,[13−16] trajectory,[17,18] and variational transition state theory[18] calculations of the rate constants of reaction 1.

Experimental Data on Reaction −1. The addition of chlorine atoms to ethylene has been studied by a number of groups.[3−11] Most of these investigations[3−7,11] were indirect studies conducted only at room temperature. Reported values of rate constants of reaction −1 are based on final product analysis, and rate constant values were obtained relative to reference reactions. The authors of refs 4−6 worked at a single fixed pressure of air or $CClF_3$. Lee and Rowland[3] reported measurements of k_{-1} at pressures of 640−4100 Torr of $CClF_3$ relative to the reaction of Cl atoms with HI. Maricq et al.[8] determined values of k_1 at room temperature and two pressures (30 and 120 Torr of nitrogen) by monitoring the real-time IR absorption of C_2H_4 following the photolysis of Cl_2. Wallington et al.[7] and Kaiser and Wallington[9] covered the widest ranges of pressures in their measurements of k_{-1} using a relative rate technique with FTIR and gas chromatographic analysis of products. Pressure ranges of these measurements extended from 10 to 3000 Torr of air[7] and from 0.2 to 100 Torr of nitrogen.[9]

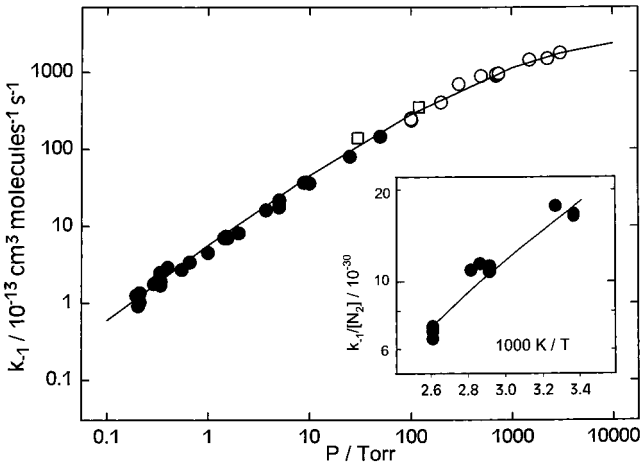

Figure 1. Plot of k_{-1} vs total pressure of air[7] or nitrogen.[8,9] Experimental points: (open circles) ref 7, (open squares) ref 8, (closed circles) ref 9. The insert shows the dependence of $k_{-1}/[N_2]$ on 1000 K/T obtained in ref 9 at 0.7 Torr of nitrogen. Lines represent the results of a master equation calculation using the selected model of reaction (1,−1) (see text).

The results indicate agreement between the rate constant values obtained using several different reference reactions. The results of these authors, together with the single-pressure measurements of refs 5 and 6 and ref 8 (which are in very good agreement with those of Wallington et al.[7]), provide a nearly complete description of falloff in nitrogen at room temperature. These measurements (Figure 1) extend from near low-pressure-limit conditions (<1 Torr) to those very close to the high-pressure limit (3000 Torr). Kaiser and Wallington[9] reported the temperature dependence of k_{-1} near the low-pressure limit (0.2−2 Torr of nitrogen) in the temperature range 297−383 K.

Recently, Stutz et al.[10] used a discharge flow technique with resonance fluorescence detection of Cl atoms at 293 K to study the kinetic isotope effect in reaction −1 at 1 Torr of helium. The value of $k_{-1} = (3.3 \pm 0.6) \times 10^{-13}$ cm^3 $molecule^{-1}$ s^{-1} agrees with one obtained in the same work by the relative rate technique. These authors reported that the rate constant obtained by the relative rate technique in nitrogen as bath gas did not differ from that obtained in helium. Finally, to address the

† Current address: Department of Chemistry, University of California, Berkeley, CA 94720.

10.1021/jp984207e CCC: $18.00
Published on Web 04/08/1999

question of the relative efficiency of helium and nitrogen as bath gas colliders, Kaiser and Wallington[11] used experimental methods analogous to those used in their earlier work[9] to study the k_{-1} pressure dependence in the range 1−5 Torr at room temperature. Their measurements confirmed the value of k_{-1} in 1 Torr of helium reported by Stutz et al. The value of k_{-1} in 1 Torr of nitrogen obtained by Kaiser and Wallington, however, was 70% higher than that determined in helium.

We present here the results of an experimental study of the unimolecular decomposition of β-chloroethyl radical, reaction 1. Rate constants for reaction 1 were measured near the low-pressure limit at five densities of helium ([He] = (3−24) × 10^{16} atoms cm^{-3}) in the temperature range 400−480 K.

Our analysis of both the new decomposition data presented here and the association data obtained earlier by other groups results in parametrized expressions describing temperature and pressure dependencies of the rate constants for reactions 1 and −1.

II. Experimental Study

CH_2CH_2Cl radicals were produced by pulsed laser photolysis and their unimolecular decay was subsequently monitored in time-resolved experiments using photoionization mass spectrometry. Details of the experimental apparatus[19] and procedures[20] used have been described before and so are only briefly reviewed here.

β-Chloroethyl radicals were produced by the pulsed, 248-nm laser photolysis of 1-chloro-2-iodoethane[21]

$$CH_2ClCH_2I \xrightarrow{248\ nm} CH_2CH_2Cl + I \qquad (2)$$

$$\rightarrow \text{other products}$$

Initial conditions (precursor concentration and laser intensity) were selected to provide low radical concentrations (less than 10^{11} molecule cm^{-3}) such that reactions between radical products had negligible rates compared to that of the unimolecular decomposition of β-chloroethyl radicals.

Pulsed unfocused 248 nm radiation (∼5 Hz) from a Lambda Physic EMG 201MSC excimer laser was directed along the axis of a heatable Pyrex reactor (1.05 cm id) lined with Teflon to reduce the rates of heterogeneous reactions. Gas flowing through the tube at ∼4 m s^{-1} contained the radical precursor (<0.02%) and an inert carrier gas (helium) in large excess. The flowing gas was completely replaced between laser pulses.

Gas was sampled through a hole (0.043 cm diameter) in the side of the reactor and formed into a beam by a conical skimmer before the gas entered the vacuum chamber containing the photoionization mass spectrometer. As the gas beam traversed the ion source, a portion was photoionized and mass selected. β-Chloroethyl radicals were ionized using the light from a chlorine resonance lamp (8.8−8.9 eV). Temporal ion signal profiles were recorded on a multichannel scaler from a short time before each laser pulse up to 20 ms following the pulse. Data from 8000 to 100000 repetitions of the experiment were accumulated before the data were analyzed.

The gases used were obtained from Lancaster (1-chloro-2-iodoethane, 97%) and Matheson (helium, >99.995%). The radical precursor was purified by vacuum distillation prior to use. Helium was used as provided.

The β-chloroethyl ion signal profiles ($m/z = 63$) were fit to an exponential function ($[CH_2CH_2Cl]_t = [CH_2CH_2Cl]_0 \exp(-k't)$) by using a nonlinear-least-squares procedure. Experiments were performed to establish that the decay constants did not depend on the initial CH_2CH_2Cl concentration (provided that the concentration was kept low enough to ensure that radical−radical reactions had negligible rates in comparison to the unimolecular reaction), the concentration of radical precursor, or the laser intensity. The exponential decay constants depended only on temperature and bath gas density.

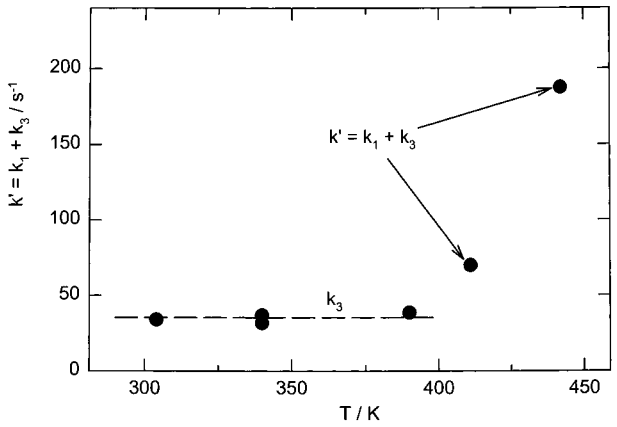

Figure 2. Plot of CH_2CH_2Cl first-order decay constants $k' = k_1 + k_3$ determined at fixed helium density ([He] = 6.0 × 10^{16} atom cm^{-3}) and several temperatures. Decay constants are independent of temperature at low temperatures but increase with temperature above 400 K due to radical decomposition. Values of k' (s^{-1}) are 34.1 at 304 K, 31.8 and 36.9 at 340 K, 38.7 at 390 K, 70 at 411 K, and 187.7 at 442 K. These data are not included in Table 1 because of higher uncertainty in the values of temperature (temperature was monitored 2 cm downstream from the sampling orifice of the reactor tube, and temperature profiles were not measured prior to conducting the experiment).

At temperatures below 350 K and helium densities in the range (3−6) × 10^{16} atom cm^{-3} the CH_2CH_2Cl decay constants (k') were low (typically 25−75 s^{-1}) and independent of temperature (Figure 2). This temperature-independent loss is attributed to heterogeneous processes:

$$CH_2CH_2Cl \rightarrow \text{heterogeneous loss} \qquad (3)$$

Above 400 K the decay constant increased rapidly with rising temperature due to the increasing importance of the thermal decomposition of the β-chloroethyl radical, reaction 1 (Figure 2). The CH_2CH_2Cl decay constants were analyzed assuming that β-chloroethyl radicals were consumed only by the two elementary reactions, 1 and 3. At low temperatures, only the heterogeneous loss (reaction 3) is observed. Above 400 K the sum of the two loss processes is observed with the CH_2CH_2Cl exponential decay constants equal to $k' = k_1 + k_3$.

Sets of experiments at 5 different fixed helium densities ((3−24) × 10^{16} atom cm^{-3}) were performed to determine k_1 as a function of temperature. The CH_2CH_2Cl exponential decay constant k′ was measured as a function of temperature keeping the helium concentration constant. Calculations of k_1 from measurements of k' require knowledge of k_3 above 350 K. While k_3 was directly determined below 350 K, it could not be measured above this temperature due to the additional loss of radicals by unimolecular decomposition. Below 350 K, k_3 was directly determined and it was found to be temperature independent at lower helium densities ((3−6) × 10^{16} atom cm^{-3}, see Figure 2). Values of k_3 above 350 K needed for the data analysis were obtained by an extrapolation assuming that k_3 retains this temperature independence up to the highest temperature of this study, 480 K. To minimize possible errors in the determination of k_3 caused by the assumed continued temperature independence above 350 K, experiments to obtain

TABLE 1: Conditions and Results of Experiments To Measure the Unimolecular Rate Constants (k_1) of the Thermal Decomposition of β-Chloroethyl Radicals

10^{-16}[He] (atoms cm^{-3})	T (K)	10^{-12} [CH_2ClCH_2I] (molecules cm^{-3})	k_3[a] (s^{-1})	k_1 (s^{-1})
3.0	440	3.2	36.3	77.3
3.0	450	3.2	36.3	120.5
3.0	450	3.1	47.9	127.4
3.0	460	3.2	36.3	157.7
3.0	470	3.2	36.3	243.7
3.0	480	3.2	36.3	321.5
6.0	420	3.1	35.3	86.7
6.0	430	3.1	35.3	133.6
6.0	440	3.1	35.3	187.0
6.0	450	3.1	35.3	250.1
6.0	460	3.1	71.3	383.7
12.0	410	3.1	38.7	99.3
12.0	420	3.1	38.7	155.3
12.0	430	3.1	38.7	269.8
12.0	430	1.7	67.3	270.4
12.0	440	3.5	66.2	382.4
18.0	410	3.1	58.0	136.3
18.0	420	3.1	58.0	235.4
18.0	430	3.5	66.2	313.9
24.0	400	3.4	24.8	112.3
24.0	400	3.3	40.1	110.3
24.0	410	3.3	40.1	180.2
24.0	420	3.3	40.1	260.7

[a] The values of k_3 were determined at lower temperatures: 350 K in experiments with [He] = (3−6) × 10^{16} atom cm^{-3} and 300 K in experiments with [He] = (12−24) × 10^{16} atom cm^{-3}. All other conditions (precursor and helium concentration, laser intensity) were kept identical in experiments to measure k_3 and k_1.

k_1 were conducted at temperatures sufficiently high to ensure that $k' > 3k_3$. It was this criterion that established the lowest temperature used to determine k_1 in each set of experiments. The highest temperature used at each total gas density was determined by the fact that decay constants above 500 s^{-1} could not be measured accurately. At higher helium densities ((12−24) × 10^{16} atom cm^{-3}) k_3 was determined at T = 300 K to avoid contribution from the decomposition which is faster at higher bath gas densities.

A potentially complicating factor in these experiments is the possible isomerization of β-chloroethyl radicals to α-chloroethyl radicals during the photolysis process. However, the α-chloroethyl radical decomposes at significantly higher temperatures than those used in the present experiments.[22] Any contribution of the α-chloroethyl radicals to the total ion signal would be revealed by a nonexponential form of the radical decay. No signs of a possible contribution of this effect were detected at temperatures of 300−480 K: chloroethyl ion signal profiles (m/z = 63) were exponential in shape and, within the accuracy of the experiments, relaxed to the original baseline in the course of the reaction.

The conditions and results of the experiments to determine k_1 are given in Table 1. The unimolecular rate constants for reaction 1 obtained from these sets of experiments are shown in Figures 3 and 4. Estimated uncertainties in the k_1 determinations vary from ± 10% in the middle of the temperature range to ±15% at the extreme temperatures used.

The determinations of k_1 reported here provide the first direct measurements of this unimolecular rate constant. The results indicate that reaction 1 is very close to the low-pressure region under the conditions of our experiments. This can be seen in Figure 4 where the second-order rate constants (k_1/[He]) are plotted. There is a good agreement between the values of (k_1/[He]) obtained at different densities of bath gas at each temperature.

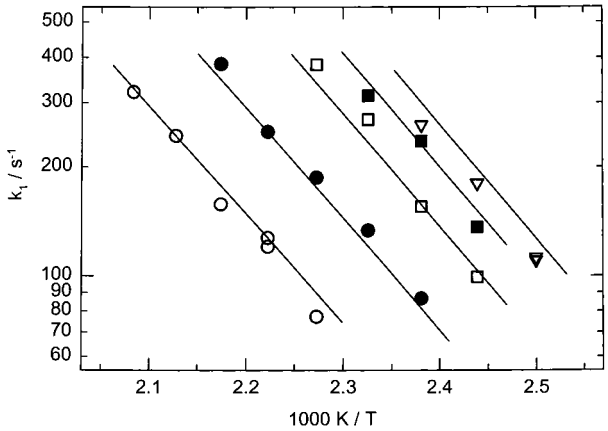

Figure 3. Plot of CH_2CH_2Cl unimolecular rate constants (k_1 vs 1000/T) for different helium densities (atoms cm^{-3}). Lines represent the results of master equation simulation using the selected model of reaction 1 (see text). (Open circles) [He] = 3 × 10^{16} atoms cm^{-3}, (closed circles) [He] = 6 × 10^{16} atoms cm^{-3}, (open squares) [He] = 12 × 10^{16} atoms cm^{-3}, (closed squares) [He] = 18 × 10^{16} atoms cm^{-3}, (open triangles) [He] = 24 × 10^{16} atoms cm^{-3}.

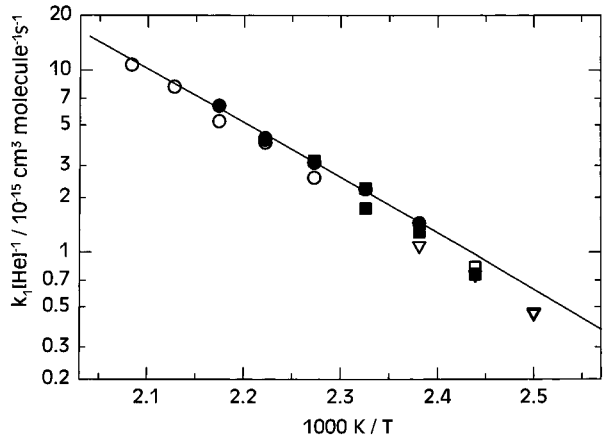

Figure 4. Arrhenius plot of the CH_2CH_2Cl decomposition rate constants displayed as bimolecular rate constants (k_1/[He]). The line represents the low-pressure-limit rate constants (k^o_1(T)) obtained in master equation simulation using the selected model of reaction 1. The deviation between the data points and the line (especially pronounced in the lower temperature and higher density end of the plot) is due to the fact that reaction 1 is not exactly in the low-pressure limit under the conditions of the experiments.

III. Discussion and Calculations

Earlier Research on the Potential Energy Surface. The molecular properties of the β-chloroethyl radical, potential energy surface of its decomposition to ethylene and chlorine atom, and reaction path for the Cl atom 1,2-migration have been investigated by several groups. Schlegel and Sosa[13] studied the dissociation process at the MP2/6-31G*//HF/6-31G* level and found a dissociation barrier with an energy 2 kJ mol^{-1} higher than that of C_2H_4 + Cl. Hoz et al.[14,15] explored the possibility of a 1,2 migration of the Cl atom employing UHF and multiconfiguration SCF procedures. Although these authors found that a symmetrically bridged structure (a potential intermediate in the 1,2-Cl-atom-migration) was higher in energy than C_2H_4 + Cl, they commented on the possibility of a migration route at larger Cl separation from ethylene, with the C−Cl distance approximately 2 times longer than typical values found in bound species.

Chen and Tschuikow−Roux[23] calculated the geometry, vibrational frequencies, and barrier for internal rotation of the CH_2CH_2Cl radical using up to the MP2/6-31G* level in the

geometry optimization, UHF/6-31G* in frequencies analysis, and up to MP4/6-311G**//MP2/6-31G* in the analysis of the internal rotation.

The most detailed ab initio study of reaction (1,−1) is that of Engels et al.[16] who conducted large-scale multireference configuration interaction calculations in a basis including polarization functions. These authors studied two possible routes of reaction (1,−1). One (nonsymmetrical) route corresponds to the Cl atom departing from the C_2H_4 fragment along the line drawn through Cl and the middle of the C−C bond. The angle between this line and the C−C bond was fixed at 50°, the value found in the equilibrium configuration of the radical. The other (symmetrical) route described the addition of the Cl atom to the double bond of ethylene following a C_{2v}-symmetry pathway with the Cl atom equidistant from both carbon atoms. Calculations[16] indicate that the first, nonsymmetric, route has a barrier of 8 kJ mol^{-1} (all energies here are cited relative to $Cl + C_2H_4$). At the same time, the second, symmetric, pathway is barrierless and leads to a shallow minimum (stable if geometry is restricted to C_{2v} symmetry) with energy of −15.5 kJ mol^{-1}. Engels et al.[16] concluded that this symmetric configuration is a transition state for the Cl atom 1,2 migration of the radical and that the minimum energy pathway for reaction 1 is a shuttling motion to this bridged symmetric configuration with a subsequent barrierless decomposition via the C_{2v} path.

One question not answered by the ab initio study of Engels et al.[16] is whether there is a barrier between the equilibrium configuration of the radical and the symmetric bridged structure corresponding to the minimum on the C_{2v} surface. Although it was implied that such a barrier does not exist and the symmetric bridged structure was described at the transition state for the shuttling motion, the text and tables of the article[16] describe only the above two reaction pathways (symmetric and nonsymmetric) and no information on the potential energy surface between them was presented. Figure 2 of ref 16 does present a potential energy surface mapped out for wide ranges of Cl atom relative coordinates. However, no individual calculated points are presented and it is not clear whether any calculations pertinent to the region of coordinates between the symmetric and nonsymmetric pathways have been performed.

Current Calculations of the Potential Energy Surface. The question of the existence or nonexistence of a barrier between the symmetric bridged structure and the absolute energy minimum is important for kinetic modeling of reaction (1,−1). Such a barrier, if present, would serve as a fixed transition state for the overall reaction. If such a barrier is not present, then reaction (1,−1) has no fixed transition state and a more complicated variational treatment[28] is appropriate. The potential energy surface calculations performed in the current work were directed at clarifying the above question of a potential energy barrier on the reaction path.

We studied the potential energy surface of reaction (1,−1) using geometry optimization at the UMP2/6-31G** level. Energy was calculated at the UMP4/6-31G** level. Spin contamination was removed by the spin projection (PMP4) method of Schlegel.[24,25] The GAUSSIAN 92 system of programs was employed.[26] Following the approach of Engels et al.,[16] two reaction paths were first investigated: (1) the C_{2v}-symmetry path with the Cl atom equidistant from the two C atoms and (2) the $\theta = 40°$ path of Engels et al.[16] Here the angle θ is formed by two lines lying in the plane of symmetry of the CH_2CH_2Cl radical and originating at the midpoint of the C−C bond (point *X* in Figure 5); one line is perpendicular to the C−C bond, the other passes through the Cl atom. θ is fixed at 40°. It was assumed that the C_s symmetry of the equilibrium structure of the radical[13,23] is preserved along the $\theta = 40°$ reaction path. In most calculations, the distance R_{XCl} between the point *X* and the Cl atom was fixed at certain values, and full geometry optimization was employed within the imposed symmetry. The coordinate system employed is that illustrated in Figure 5.

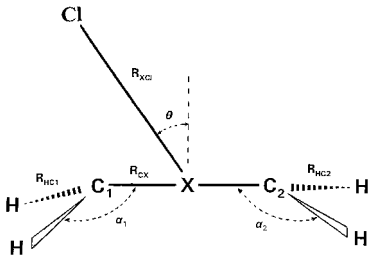

Figure 5. The coordinate system used in the present study of the potential energy surface of the reaction (1,−1). Point *X* is the center of the line connecting the two carbon atoms. Parameters are: R_{XCl} (*X*−Cl distance), R_{CX} (C-*X* distance, one-half of C_1-C_2 distance), R_{HC_i} (H−C_i distance, $i = 1, 2$), θ ($\theta = 90°$ minus Cl−*X*−C_1 angle), α_i (angle H−C_i−*X*, $i = 1, 2$), β_i (dihedral angle H−C_i−*X*−Cl; $i = 1, 2$, where H is bound to C_i; β is not shown in the figure). Cl lies in the plane of symmetry of the CH_2CH_2Cl molecule.

At the UMP4/6-31G**// UMP2/6-31G** level, the results for these two reaction paths are in general agreement with those of Engels et al.[16] An absolute potential energy minimum (conformation **1**) was found at $\theta = 39.57°$ and $R_{XCl} = 2.196$ Å (which explains the choice of the fixed value $\theta = 40°$ for the nonsymmetric reaction pathway). A barrier (conformation **2**) of 13.5 kJ mol^{-1} relative to $Cl + C_2H_4$ was found in the reaction path with $\theta = 40°$. The C_{2v}-symmetry reaction path has a shallow minimum (−18.2 kJ mol^{-1}, conformation **3**) and no barrier for separation of Cl and C_2H_4. The UMP2/6-31G** vibrational frequencies of conformation **3** are positive indicating that it is a stable configuration. The transition state between structures **1** and **3** was found at $\theta = 15.78°$ and $R_{XCl} = 2.48$ Å (conformation **4**). Its UMP4/6-31G** energy is 3.7 kJ mol^{-1} below the energy of the separated fragments and 14.5 kJ mol^{-1} above that of conformation **3**.

Removal of spin contamination by the PMP4 method,[24,25] however, results in significant qualitative changes of the potential energy surface. While the potential energy profile along the symmetric path remains the same, barriers corresponding to conformations **2** and **4** disappear. The PMP4/6-31G**//UMP2/6-31G** energy of conformation **2** ("transition state" for the nonsymmetric path) is 6.6 kJ mol^{-1} below the energy of separated Cl and C_2H_4 and that of conformation **4** (the "transition state" between **1** and **3**) is 1.4 kJ mol^{-1} below the minimum on the C_{2v} path (conformation **3**). Detailed information on the structures and energies of conformations **1**−**4**, as well as a plot of potential energy profiles along the symmetric and the nonsymmetric paths, are presented in the Supporting Information.

The results of the current ab initio study of reaction (1,−1) confirm the statement by Engels et al.[16] that the symmetric bridged structure on the C_{2v} surface is the transition state for the Cl atom 1,2 migration and that the β-chloroethyl radical decomposition proceeds first via the formation of this bridged structure and then along the symmetric pathway to Cl and C_2H_4. The main difference between the current work and that of Engels et al. is that, at the PMP4 level, we did not find the barrier for decomposition via the nonsymmetric path with $\theta = 40°$ reported by these authors. One possible reason for this disagreement is that Engels et al. used only partial optimization of geometry. In their calculations, the $-CH_2$ group of CH_2CH_2Cl radical was frozen with bond lengths and angles equal to those of ethylene.[16]

Master Equation Modeling of Reaction (1,−1) and Parametrization of Rate Constants. Modeling of the dynamics and kinetics of reaction 1 has been attempted by several groups. Sewell et al. analyzed the dynamics of the unimolecular decomposition of the β-chloroethyl radical using classical trajectory calculations[17,18] and variational transition state theory.[18] However, these authors employed a potential energy surface model which assumed a barrier for addition of Cl to C_2H_4 and ignored the symmetrical path. Barat and Bozzelli[27] recommended Arrhenius parameters for reaction 1 ($k_1^\infty = 3.9 \times 10^{13}$ exp($-10920\ K/T$) s^{-1}) on the basis of thermochemical estimates. Their model, however, is incompatible with the findings of Engels et al.[16] and of the current ab initio study, since it includes a 1 kcal mol^{-1} barrier for the addition of Cl atom to ethylene.

As follows from the results of ab initio studies (ref 16 and the current work), reaction 1 proceeds through the symmetric bridged structure with subsequent decomposition via the C_{2v}-symmetry path. The reaction has no barrier. Rigorous quantitative modeling of such a reaction requires an application of microcanonical variational transition state theory[28] where the position of the transition state along the reaction coordinate depends on both the vibrational energy (E) and angular momentum (J) of the molecule. A description of the pressure dependence requires the solution of a two-dimensional master equation (E and J dependent)[28] describing an interplay between the reaction and collisional relaxation in both vibrational and rotational energy manifolds. Such modeling requires full and accurate knowledge of the multidimensional reaction potential energy surface in the transition state region, information which is not currently available.

In view of this lack of information, as well as the absence of established models of collisional energy transfer in rotational degrees of freedom, we did not attempt a rigorous modeling of reaction (1,−1). Instead, a simplified model was created with the purpose of fitting the available kinetic data on both direct and reverse reactions in order to provide parametrized expressions for rate constants outside the experimental conditions. A fixed (independent of energy) transition state was assumed to be located on the symmetric part of the reaction path. The choice of the transition state geometry was guided by selecting the Cl − C_2H_4 separation distance (3.4 Å) at which the calculated PMP4 level energy (−9.0 kJ mol^{-1}) relative to products is approximately equal to the negative activation energy of −8.9 kJ mol^{-1} obtained from the k_{-1} vs T dependence at 0.7 Torr of nitrogen reported in ref 9. This choice of transition-state structure resulted in rotational constants of 0.0882 cm^{-1} (2-dimensional inactive rotation) and 0.830 cm^{-1} (one-dimensional active rotation). Rate constants were obtained by solving a steady-state one-dimensional (in energy only) master equation[28]

$$-k_1 g(E) = \omega \int_0^\infty [P(E,E')g(E') - P(E',E)g(E)]\mathrm{d}E' - k(E)g(E)$$

where $g(E)$ is the steady-state energy distribution of CH_2CH_2Cl molecules, ω is the frequency of collisions with the bath gas, E is energy, $k(E)$ are the energy-dependent microscopic rate constants for the radical decomposition, and $P(E,E')$ is the density of probability of collisional energy transfer from energy E' to energy E. The exponential-down model[28,29] of the collisional energy transfer was used:

$$P(E,E') = A \exp[-(E' - E)/\alpha] \text{ (for } E' > E)$$

where A is a normalization constant and α is a quantitative characteristic of the "width" of the $P(E,E')$ distribution, a constant which coincides with $\langle\Delta E\rangle_{down}$ (the average energy transferred in downward collisions with the bath gas) for all energies $E' \gg \alpha$. The master equation was solved using the algorithm of Gaynor et al.[28,30] Energy-dependent rate constants were calculated using the RRKM method.[28,31] Densities and sums of states were calculated using the modified Beyer−Swinehart algorithm.[32] The hindered rotor in CH_2CH_2Cl was treated classically using the formalism of Knyazev et al.[33] To approximately account for angular momentum conservation, a method introduced by Marcus[34] was used (see refs 31 and 21 for a more detailed description of the method). Properties of Cl and C_2H_4 were taken from refs 35 and 36 and those of CH_2CH_2Cl from the ab initio study of Chen and Tschuikow−Roux.[23] The heat of formation of the β-chloroethyl radical, $\Delta H_f^\circ{}_{298}(CH_2CH_2Cl) = 97.5 \pm 3.0$ kJ mol^{-1}, was taken from the third-law analysis of Seetula[37] based on experimental data on the $CH_2CH_2Cl + HBr \rightleftarrows CH_3CH_2Cl + Br$ reaction. The resultant 0 K energy difference between CH_2CH_2Cl and $Cl+C_2H_4$ is $E_{1,-1} = 74.8$ kJ mol^{-1} (zero-point vibrational energy of the hindered rotation is not included to enable classical treatment).

The energy threshold of reaction 1, E_1 ($E_1 = 70.7$ kJ mol^{-1}), and $\langle\Delta E\rangle_{all}$ in helium as bath gas ($\langle\Delta E\rangle_{all}$(He) = −37 cm^{-1}) were adjusted to reproduce the experimental values of $k_1(T,[He])$ obtained in the current study and the value of $k_{-1} = 3.3 \times 10^{-13}$ cm^3 $molecules^{-1}$ s^{-1} at 293 K and 1.0 Torr of helium reported by Stutz et al.[10] and confirmed by Kaiser and Wallington.[11] Here, $\langle\Delta E\rangle_{all}$ is the average energy transferred per collision with bath gas in both upward and downward transitions.[28] The value of $\langle\Delta E\rangle_{all}$ in nitrogen as bath gas ($\langle\Delta E\rangle_{all}(N_2)$= −115 cm^{-1}) was selected to reproduce the experimental k_{-1} vs T dependence at 0.7 Torr of nitrogen reported by Kaiser and Wallington[9] (Figure 1). Twelve frequencies of the transition state were taken as equal to those of ethylene, and the remaining two frequencies of the tumbling motion of the C_2H_4 fragment relative to the Cl atom were adjusted to reproduce the values of k_{-1} at the three highest pressures (>1000 Torr) of Wallington et al.[7] ($\nu_{13} = \nu_{14} = 50$ cm^{-1}). The resultant simplified model of reaction (1,−1) yields rate constant values which are in good agreement with the experimental data (Figures 1 and 3).

We present here a parametrization of k_1 and k_{-1} in helium and nitrogen which provides rate constant values throughout the range of temperatures 200−800 K and pressures $0.1-1 \times 10^4$ Torr. The modified Lindemann−Hinshelwood expression introduced by Gilbert et al.[38] was used. Values of k_1 and k_{-1} in the above temperature and pressure intervals were calculated using the master equation/RRKM approach with the simplified model of the reaction presented above. The following temperature dependencies of the high- and low-pressure-limit rate constants were obtained:

$$k^\infty{}_1 = 1.66 \times 10^{14} \exp(-8763\ K/T)\ s^{-1}$$

$$k_1{}^0(\mathrm{He}) = 3.98 \times 10^9 T^{-5.61} \exp(-9413\ K/T)\ cm^3\ molecule^{-1}\ s^{-1}$$

$$k_1{}^0(N_2) = 2.25 \times 10^9 T^{-5.43} \exp(-9369 K/T)\ cm^3\ molecule^{-1}\ s^{-1}$$

$$k^\infty{}_{-1} = 2.96 \times 10^{-14} T^{1.31} \exp(518\ K/T)\ cm^3\ molecule^{-1}\ s^{-1}$$

The matrix of calculated values of rate constants was fitted with the modified Lindemann−Hinshelwood expression,[38] and the resulting values of F_{cent} (a general center broadening factor[38])

are $F_{cent}(He) = 0.467$ and $F_{cent}(N_2) = 0.505$ (independent of temperature). The average deviation of fit is 8% and maximum deviation is 19%. The upper temperature limit of the rate constant parametrization is determined by the significance of non-steady-state effects[39,40] above 800 K where the notion of a time-independent rate constant is inapplicable.

This parametrization is most reliable under the conditions of the experiments on the results on which the model of reaction 1,−1 was based, that is, room temperature for the predicted k_{-1} values and $T = 400-480$ K and low pressures for k_1. One should bear in mind that the above model of the reaction is based on significant simplifications and that the available experimental data are not sufficient to specify all the parameters of even the simplified model. In particular, different temperature dependencies of the collisional parameters and a different (within uncertainties) heat of formation of CH_2CH_2Cl will result in different values of rate constants. Moreover, the simplifications of the model (e.g., the assumption of a fixed transition state and the representation of the tumbling motion of the C_2H_4 fragment relative to the Cl atom in the transition state with low-frequency vibrational modes) result in uncertainties which are not easily estimated. Therefore, because of the large uncertainties in the parameters of the model, caution is advised in using the results of this extrapolation far outside the corresponding ranges of conditions.

Acknowledgment. This research was supported by the National Science Foundation, Division of Chemical, Biochemical and Thermal Engineering under Grant CTS-9311848. The authors thank Drs. E. W. Kaiser and T. J. Wallington for sharing their experimental data.

Supporting Information Available: Supplement describing the results of the ab initio study of reaction (1,−1) (four pages). Table 1S containing information on the properties of several conformations on the potential energy surface. Figure 1S describing potential energy surface scans. Supporting Information is free of charge via the Internet at http://pubs.acs.org.

References and Notes

(1) Tsang, W. *Combust. Sci. Technol.* **1990**, *74*, 99.
(2) Keene, W. C.; Jacob, D. J.; Fan, S. *Atmos. Environ.* **1996**, *30*, No. 6, i.
(3) Lee, F. S. C.; Rowland, F. C. *J. Phys. Chem.* **1977**, *81*, 1235.
(4) Iyer, S. R.; Rogers, P. J.; Rowland, F. S. *J. Phys. Chem.* **1983**, *87*, 3799.
(5) (a) Atkinson, R.; Aschmann, S. M. *Int. J. Chem. Kinet.* **1985**, *17*, 33. (b) Atkinson, R.; Aschmann, S. M. *Int. J. Chem. Kinet.* **1987**, *19*, 1097.
(6) Wallington, T. J.; Skewes, L. M.; Siegl, W. O. *J. Photochem. Photobiol.* **1988**, 45, 167.
(7) Wallington, T. J.; Andino, J. M.; Lorkovic, I. M.; Kaiser, E. W.; Marston, G. *J. Phys. Chem.* **1990**, *94*, 3644.
(8) Maricq, M. M.; Szente, J. J.; Kaiser, E. W. *J. Phys. Chem.* **1993**, *97*, 7970.
(9) Kaiser, E. W.; Wallington, T. J. *J. Phys. Chem.* **1996**, *100*, 4111.
(10) Stutz, J.; Ezell, M. J.; Finlayson-Pitts, B. J. *J. Phys. Chem. A* **1997**, *101*, 9187.
(11) Kaiser, E. W.; Wallington, T. J. *J. Phys. Chem. A* **1998**, *102*, 6054.
(12) (a) Dobis, O.; Benson, S. W. *J. Am. Chem. Soc.* **1991**, *113*, 6377. (b) Pilgrim, J. S.; Taatjes, C. A. *J. Phys. Chem. A* **1997**, *101*, 4172.
(13) Schlegel, H. B.; Sosa, C. *J. Phys. Chem.* **1984**, *88*, 1141.
(14) Hoz, T.; Sprecher, M.; Basch, H. *Isr. J. Chem.* **1983**, *23*, 109.
(15) Hoz, T.; Sprecher, M.; Basch, H. *J. Phys. Chem.* **1985**, *89*, 1664.
(16) Engels, B.; Peyerimhoff, S. D.; Skell, P. S. *J. Phys. Chem.* **1990**, *94*, 1267.
(17) Sewell, T. D.; Thompson, D. L. *J. Chem. Phys.* **1990**, *93*, 4077.
(18) Sewell, T. D.; Schranz, H. W.; Thompson, D. L.; Raff, L. M. *J. Chem. Phys.* **1991**, *95*, 8089.
(19) Slagle, I. R.; Gutman, D. *J. Am. Chem. Soc.* **1985**, *107*, 5342.
(20) (a) Slagle, I. R.; Batt, L.; Gmurczyk, G.; Gutman, D.; Tsang, W. *J. Phys. Chem.* **1991**, *95*, 7732. (b) Knyazev, V. D.; Slagle, I. R. *J. Phys. Chem.* **1996**, *100*, 5318.
(21) Minton, T. K.; Felder, P.; Brudzynski, R. J.; Lee, Y. T. *J. Chem. Phys.* **1984**, *81*, 1759.
(22) Knyazev, V. D.; Bencsura, A.; Dubinsky, I. A.; Gutman, D.; Senkan, S. M. *Int. Proc. Symp. Combust.* **1994**, *25*, 817.
(23) Chen, Y.; Tschuikow-Roux, E. *J. Phys. Chem.* **1992**, *96*, 7266.
(24) Schlegel, H. B. *J. Chem. Phys.* **1986**, *84*, 4530.
(25) Schlegel, H. B. *J. Phys. Chem.* **1988**, *92*, 3075.
(26) Frisch, M. J.; Trucks, G. W.; Head-Gordon, M.; Gill, P. M. W.; Wong, M. W.; Foresman, J. B.; Johnson, B. G.; Schlegel, H. B.; Robb, M. A.; Replogle, E. S.; Gomperts, R.; Andres, J. L.; Raghavachari, K.; Binkley, J. S.; Gonzalez, C.; Martin, R. L.; Fox, D. J.; Defrees, D. J.; Baker, J.; Stewart, J. J. P.; Pople J. A. *Gaussian 92*, Revision E.1; Gaussian, Inc.: Pittsburgh, PA, 1992.
(27) Barat, R. B.; Bozzelli, J. W. *J. Phys. Chem.* **1992**, *96*, 2494.
(28) Gilbert, R. G.; Smith, S. C. *Theory of Unimolecular and Recombination Reactions*; Blackwell: Oxford, 1990.
(29) Rabinovitch, B. S.; Tardy, D. C. *J. Chem. Phys.* **1966**, *45*, 3720.
(30) Gaynor, B. J.; Gilbert, R. G.; King, K. D. *Chem. Phys. Lett.* **1978**, *55*, 40.
(31) Robinson, P. J.; Holbrook, K. A. *Unimolecular Reactions*; Wiley-Interscience: New York, 1972.
(32) Astholz, D. C.; Troe, J.; Wieters, W. *J. Chem. Phys.* **1979**, *70*, 5107.
(33) Knyazev, V. D.; Dubinsky, I. A.; Slagle, I. R.; Gutman, D. *J. Phys. Chem.* **1994**, *98*, 5279.
(34) Marcus, R. A. *J. Chem. Phys.* **1965**, *43*, 2658.
(35) Chase, M. W., Jr.; Davies, C. A.; Downey, J. R., Jr.; Frurip, D. J.; McDonald, R. A.; Syverud, A. N. *JANAF Thermochemical Tables, 3rd ed.*, *J. Phys. Chem. Ref. Data, Suppl.* **1985**, *14* (1).
(36) Chao, J.; Zwolinski, B. J. *J. Phys. Chem. Ref. Data* **1975**, *4*, 251.
(37) Seetula, J. A. *J. Chem. Soc., Faraday Trans.* **1998**, *94*, 891.
(38) Gilbert, R. G.; Luther, K.; Troe, J. *Ber. Bunsen-Ges. Phys. Chem.* **1983**, *87*, 169.
(39) Bernshtein, V.; Oref, I. *J. Phys. Chem.* **1993**, *97*, 6830.
(40) Tsang, W.; Bedanov, V.; Zachariah, M. R. *J. Phys. Chem.* **1996**, *100*, 4011.